Analysis of HRT Images: Comparison of Reference Planes

Alessandro Poli,[1,2,3] *Nicholas G. Strouthidis,*[1] *Tuan A. Ho,*[1] *and David F. Garway-Heath*[1,3]

Purpose. The values of Heidelberg Retinal Tomograph (HRT; Heidelberg Engineering, Heidelberg, Germany) stereometric parameters depend on the reference plane (RP), the instability of which results in parameter variability. Identification of change depends on RP stability. This study was undertaken to evaluate the influence of various RPs on rim areas (RAs) in a longitudinal image series.

Methods. A longitudinal image series of 31 subjects with ocular hypertension who had reproducible visual field loss and 19 normal subjects was analyzed using five different RPs: the standard RP (HRT software version 3.1.2.0), two 320-μm RPs (software ver. 3.1.2.0 and 1.7.0), a previously described experimental RP, and a new Moorfields RP. The Moorfields RP takes the standard RP at baseline and then is fixed relative to the reference ring for subsequent images. Linear regression of RA over time was performed, and the slope and residual SD (RSD) were calculated for each RP. Comparisons between RPs were made by paired *t*-tests.

Results. In eyes with progressing disease, application of the standard RP resulted in significantly greater variability (as measured by the RSD) compared with other RPs (mean 0.057 mm^2 vs. 0.035–0.038 mm^2). There was a trend toward faster RA change/time (mean, -0.0123 mm^2/y) for the standard RP and slower (-0.0095 mm^2/y) for the experimental RP. There was a trend for the Moorfields RP to result in the best signal-to-noise ratio (speed of RA change/variability): mean RA slope -0.0118 mm^2/y and mean global RSD 0.037mm^2.

Conclusions. Compared to the standard RP, the Moorfields RP has significantly lower variability and probably provides a greater facility for discriminating RA change from measurement variability in a longitudinal HRT image series. (*Invest Ophthalmol Vis Sci.* 2008;49:3970–3975) DOI:10.1167/iovs.08-1764

From the [1]National Institute for Health Research Biomedical Research Centre for Ophthalmology, Moorfields Eye Hospital NHS (National Health Service) Foundation Trust and the UCL Institute for Ophthalmology, London, United Kingdom; the [2]University Eye Clinic, Verona, Italy; and the [3]GB Bietti Foundation for Research in Ophthalmology, IRCCS (Istituto Ricerca e Cura a Carattere Scientifico) Rome, Italy.

Supported by Carl Zeiss Meditec, Heidelberg Engineering, and Optovue. DFG-H has received a proportion of his funding from the Department of Health's National Institute for Health Research Biomedical Research Centre at Moorfields Eye Hospital and the UCL Institute of Ophthalmology. The views expressed in this publication are those of the authors and not necessarily those of the Department of Health, United Kingdom.

Submitted for publication January 19, 2008; revised March 16 and April 10, 2008; accepted July 21, 2008.

Disclosure: **A. Poli**, None; **N.G. Strouthidis**, None; **T.A. Ho**, None; **D.F. Garway-Heath**, Carl Zeiss Meditec (F, C), Optovue (F, C), Heidelberg Engineering (F)

The publication costs of this article were defrayed in part by page charge payment. This article must therefore be marked "*advertisement*" in accordance with 18 U.S.C. §1734 solely to indicate this fact.

Corresponding author: David F. Garway-Heath, Glaucoma Research Unit, Moorfields Eye Hospital, City Road, London EC1V 2PD; david.garway-heath@moorfields.nhs.uk.

Morphologic changes at the optic nerve head (ONH) are a key feature of glaucoma. Qualitative and quantitative assessments of the ONH are established methods of detecting the disease[1,2] and identifying progression.[3,4] Classic methods, such as ophthalmoscopy and stereophotography, are widely used and are still important. These techniques involve the clinical examination of the ONH, to detect abnormalities associated with glaucoma, such as rim narrowing and notching, and recognition of large or asymmetric cup-to-disc ratios. However, these methods have limitations, since they rely on subjective judgment, and agreement between even expert observers on the presence of glaucoma or progressive change is not optimal.[5–10] Objective and reproducible measurements of the ONH surface topography are possible with scanning laser tomography.[11,12] Although scanning laser tomography appears to be reproducible,[13] it is difficult to manage the large amount of data in the images to generate clinically useful information regarding change over time.

The HRT software applies two approaches to detection of change. The first is topographic change analysis,[14] in which the surface height in groups of pixels (super pixels) in follow-up images is compared with the surface height in the baseline image. Statistically significant change in surface height is color coded (red for relative depression, and green for relative elevation, compared to baseline). The second approach is to plot stereometric data, such as rim area (RA), over time. Currently, there is no statistical support in the software for this latter approach, but the potential value of quantifying RA over time to identify progression has been reported.[15–21] To generate stereometric parameter values, such as RA, an RP (below, and parallel to, the parapapillary retinal surface) must be placed in the topographic image. The stereometric parameters depend heavily on the position of this plane, and it is crucial that it maintain a fixed position in relation to the tissue of interest for stereometric parameter measurements to be reproducible. Fluctuation in the relative positions of the ONH surface and the RP causes a fluctuation in RA values,[13,22–24] which may mimic or mask glaucomatous progression.

Many different reference surfaces have been proposed.[25,26] Early versions of the Heidelberg Retina Tomograph (HRT; Heidelberg Engineering, Heidelberg, Germany) software used a curved reference surface. However, this was replaced by flat reference planes,[25] and various landmarks have been proposed for their positioning, such as peripapillary sclera,[27,28] retinal pigment epithelium (Tuulonen A, et al. *IOVS* 1993;34:ARVO Abstract 1729), peripapillary retina,[29,30] and retinal height at the margin of the ONH.[25,29]

RA is one of the most reproducible stereometric parameters,[16,17] distinguishes well between normal and glaucomatous subjects[31] and is useful in identifying progression.[16,17] It also has the advantage of being familiar to clinicians. The purpose of this study was to investigate the effect of various RP definitions on RA values in subjects without risk factors for glaucoma (presumed stable) and in those with risk factors for glaucoma

Investigative Ophthalmology & Visual Science, September 2008, Vol. 49, No. 9
Copyright © Association for Research in Vision and Ophthalmology

Downloaded from iovs.arvojournals.org on 06/30/2019

Table 1. Demographics of Normal and Converter Subjects

	Normal	Converter
Subjects (*n*)	19	31
Age (y)*	65.7 ± 8.5 (42–70)	62.7 ± 10.9 (43–75)
Examinations (*n*)	10.3 (8–14)	10.7 (7–15)
Follow-up (y)*	5.7 ± 1.28 (3.5–7.0)	6.4 ± 0.9 (4.0–7.1)
Laterality (*n*, right:left)	10:9	18:13

* Mean ± SD.

(ocular hypertension) who demonstrated visual field (VF) progression.

Methods

Subjects

This was a retrospective analysis of images acquired in subjects with ocular hypertension taking part in a clinical trial[32] and normal subjects, without risk factors for glaucoma,[33] under observation in the Glaucoma Research Unit at Moorfields Eye Hospital. The two cohorts of subjects comprised 31 converters and 19 normal subjects (both defined later). The demographics of the subjects identified for this study are summarized in Table 1. All subjects were imaged with the HRT during a 7-year follow-up (1994–2001) and had undergone HRT imaging and perimetry at least six times. Different operators with various levels of experience had acquired the images because of turnover in research clinic technical staff over the period. The study adhered to the tenets of the Declaration of Helsinki and had appropriate institutional review board approval and the subjects' informed consent.

Normal subjects were volunteers: spouses or friends of hospital patients, hospital staff, or members of external nonmedical social organizations. They had IOP persistently less than 22 mm Hg, normal and reliable serial visual field (VF) results (Humphrey 24-2; Carl Zeiss Meditec, Inc, Dublin, CA), with an Advanced Glaucoma Intervention Study (AGIS) score of 0, no concurrent ocular disease, no family history of glaucoma, and refractive error less than 6 D. All were older than 40 years. The appearance of the ONH was not taken into account for entry into the study.

Converters initially had a diagnosis of ocular hypertension (IOP > 22 mm Hg); open angles on gonioscopy, refractive error less than 6 D, and no concurrent ocular disease and were older than 40 years. All had initially normal VF results (Humphrey 24- 2; AGIS score = 0) and began to show VF defects during the course of monitoring (AGIS VF score changed from 0 to >1 in three consecutive VF examinations, with the defect at the same test-point location).

Image Acquisition

Images were acquired with the HRT classic (from 1994–2001). Three well-centered 10° single topography images were acquired at each session, without pupil dilatation.

Image Analysis

Three changes in the most recent version of the HRT3 software have the potential to improve the reproducibility of stereometric parameter measurements: improved image alignment, revised rules defining the position of the peripheral reference ring, and display of regions in the mean topography for which there is not complete overlap of component single topography images (this has the effect of increasing the imaged area in cases in which ONH centration varies in the component single topographies). The reference ring is the zero-referencing region for pixel heights.[25] It is centered on the image frame and located in its periphery with an outer diameter of 94% and a width 3% of the image size. In previous versions of the software, for analysis of image series, the reference ring was positioned in the outer limit of the region of the follow-up image for which there was complete overlap with the baseline image (Fig. 1, top). Thus, the reference ring could vary in size and position from one follow-up image to another, depending on the degree of overlap with the baseline image. In the new version of the software, the reference ring's diameter is adapted according to the total region of the image (in which there may not be complete overlap of the component single topography images).

The baseline reference ring is aligned to retinal features so that its position is constant in the follow-up images (Fig. 1, bottom). If differences in ONH centration in follow-up images cause the reference ring to fall outside the imaged area, the region of the reference ring outside the image is given null height values and is not take into account in any calculations (Reutter M, Heidelberg Engineering, personal communication, 2008).

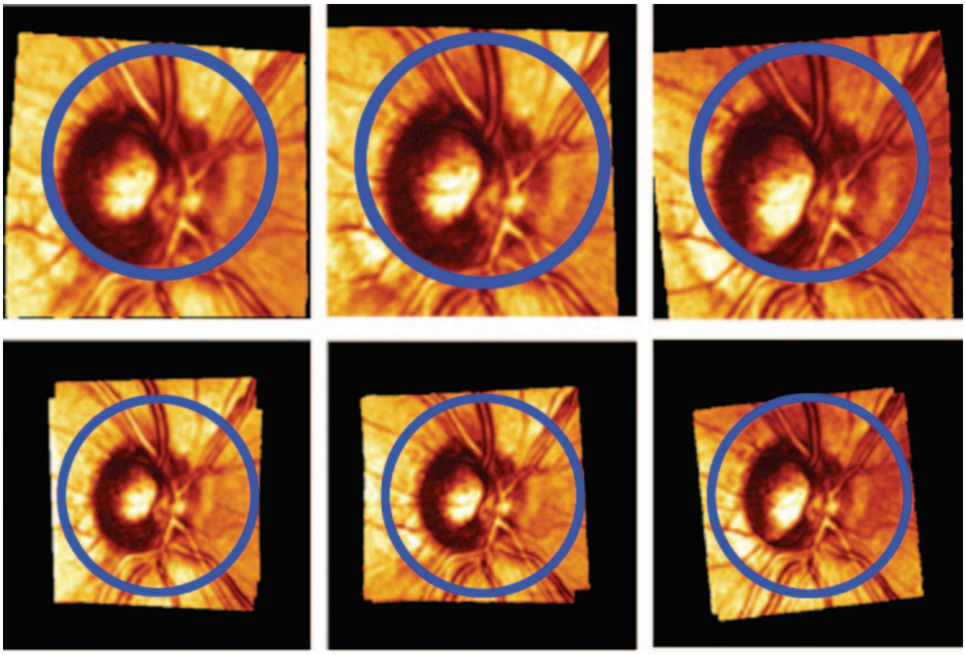

Figure 1. Illustration of peripheral reference ring position in a series of images with limited overlap of imaged region during follow-up. *Top*: Explorer, ver. 1.7.0; *bottom*: Explorer, ver. 3.1.2.0 (Heidelberg Engineering, Heidelberg, Germany).

Downloaded from iovs.arvojournals.org on 06/30/2019

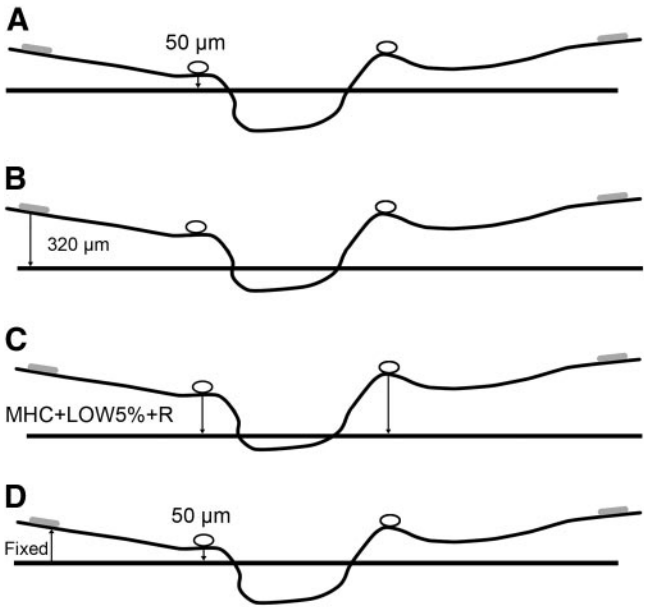

FIGURE 2. Position of various RPs relative to the parapapillary retinal surface and optic nerve head. *Filled symbols*: the reference ring position; *open symbols*: the contour line position. (**A**) Standard RP, (**B**) 320-μm RP, (**C**) experimental RP, (**D**) Moorfields RP.

Mean topography images from the converting eye in each of the subjects in the converter group and a randomly selected eye from each of the normal subjects were generated from triplets of single topography images which were acquired with the HRT Classic device. Images were processed in HRT-3 software (version 3.1.2.0) customized by the manufacturer to allow the application of the various reference planes, as well as an older version of the software (ver. 1.7.0), to enable analysis using the 320-μm RP without the new alignment algorithm. Mean topographies with a mean pixel SD worse than 50 μm were excluded. An ONH margin contour line was drawn corresponding to the inner margin of Elschnig's ring on the baseline mean topographic image of each subject. RA was calculated globally and regionally (six machine-defined sectors).

The software applies the same disc margin contour line to each image, permitting an exact comparison of RA generated with each reference plane.

The five RPs examined were as follows:

1. *Standard RP*: the RP implemented in current versions of HRT software. It is fixed 50 μm posterior to the mean contour line height between 350° and 356° at the temporal ONH margin.
2. *320-μm RP OLD*: a plane fixed 320 μm posterior to the reference ring, as used in older versions of the software (HRT ver. 1.7.0 and earlier).
3. *320-μm RP NEW*: a fixed 320 μm posterior to the reference ring, using the HRT-3 software (ver. 3.1.2.0) with the new alignment algorithm.
4. *Experimental RP*: a plane that was proposed by Tan and Hitchings.[26] For each eye, a mean topography image was selected to be the baseline image in which the position of the RP was determined, calculating the position as follows:
   - LOW5%. The contour line's lowest region (LOW5%) was calculated. Heights 1° apart (360 data points) on the contour lines of single topography images (used to derive the baseline mean topography image) were read from the HRT software. Heights were ranked in each single topography image, from which the mean of the lowest 5% of heights was calculated. The means of the lowest 5% of heights for each of the three single topography images were averaged to arrive at LOW5%.
   - R. The RP was positioned to ensure that it lay beneath the entire circumference of the contour line. An RP lying above part of the contour line underestimates adjacent rim tissue. To determine R, variability was analyzed in a longitudinal image series of normal control eyes. R was the distance of the RP beneath LOW5%, where RA variability was the least and was held constant once calculated.
   - REFdis. Once positioned at R, the *z*-axis distance of the RP below mean height of the contour line (MHC; which is the mean height of locations on the contour line measured in relation to the reference ring) was calculated for each ONH and called REFdis. MHC was used as a marker of the topographical *z*-axis position of the ONH. REFdis is unique to each ONH and, once calculated in the baseline image, is kept constant in all the images of an eye. By keeping REFdis constant, the height relationship between the ONH and RP was kept constant in image series of the same eye. REFdis can be expressed as: REFdis = LOW5% + R.
   - REFpos. Position of the RP, or REFpos, can thus be expressed as: MHC + REFdis = MHC + LOW5% + R.
5. *Moorfields RP*: the standard RP is applied in the baseline image, and the height difference between the baseline RP and the reference ring is calculated and kept constant for follow-up images.

The relative positions of the five RPs are illustrated in Figure 2.

Data Analysis

All statistical analyses were performed with commercial software (Medcalc ver. 7.4.2.0; Medcalc Software, Mariakerke, Belgium). Linear regression analyses of RA/time were performed for each longitudinal series of images, at each of the five RPs. Variability of the series was estimated by using residual SD (RSD) of the RA, for each RP, from the regression analyses. Residuals are derived from the differences between observed (y_{obs}) and predicted values (y_{est}). RSD is calculated from the SE of estimates (SE_{yx}) as:

$$SE_{yx} = \sqrt{[\Sigma\,(y_{obs} - y_{est})^2/(n-2)]}.$$

Since it is of primary importance that a glaucoma tool have the capability of detecting progressive changes, unimpeded by measurement variability, the ratio between the slope and RSD (slope/RSD) was calculated.

All the results were compared by means of paired *t*-test with significance assumed at a level of 5% ($P < 0.05$).

Results

Converters

The Standard RP demonstrated the highest rate of RA change over time and the experimental the lowest (Table 2). The Moorfields RP had a steeper slope than did the experimental and the 320-μm RPs (320 RPs), although the difference was not

TABLE 2. Mean Baseline RA and Mean Slope of RA/Time at Each RP in the Converter Cohort

RP	Mean Baseline RA (mm^2)	Mean Slope RA (mm^2/y)	Mean Slope RA (%/y)
Standard	1.155	−0.0123	−1.06
Experimental	1.356	−0.0095	−0.77
Moorfields	1.155	−0.0118	−0.99
320 New	1.157	−0.0100	−0.82
320 Old	1.162	−0.0096	−0.82

Downloaded from iovs.arvojournals.org on 06/30/2019

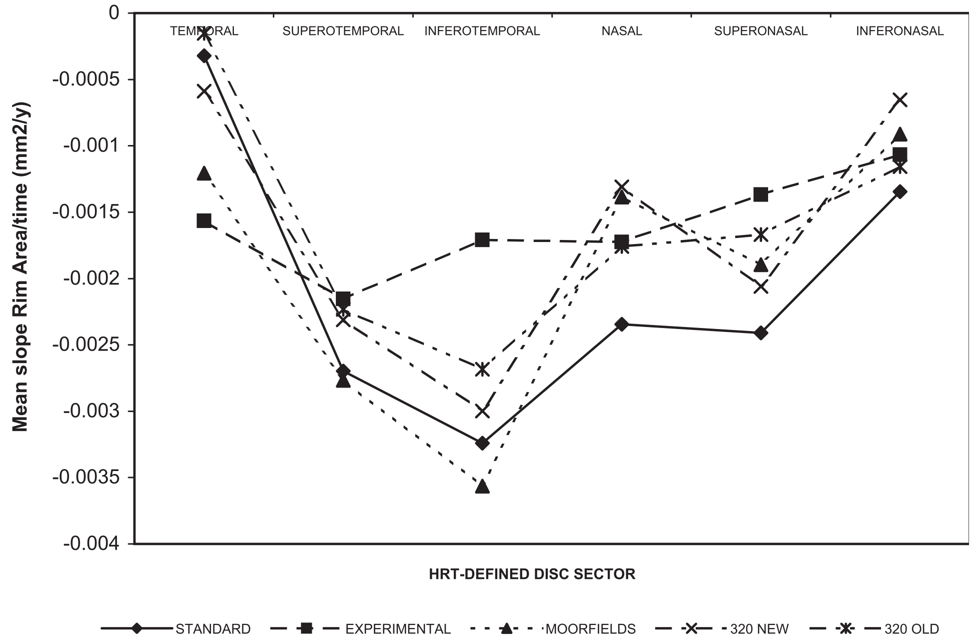

FIGURE 3. The rate of sector rim area change/time for each RP in the converter group.

statistically significant. The rate of change was higher in the superior and inferior sectors of the ONH for every RP (Fig. 3).

The standard RP resulted in the greatest variability (highest global RA RSD), whereas the experimental RP resulted in the lowest (Table 3). The RSD with the Moorfields RP closely approximated that of the 320 RPs (as expected). The difference in RSD between the standard RP and the others was statistically significant (Table 3). Each RP had lower RSDs in the nasal/inferior sectors and higher RSDs in the temporal sectors (Fig. 4).

The standard RP had the lowest slope/RSD, indicating a relatively lower facility for identifying change (i.e., lowest signal-to-noise ratio). The Moorfields RP had the best performance (highest signal-to-noise ratio), although the differences between RPs was not statistically significant (Table 4).

Normal Group

In the normal group, it is assumed that RA should be stable over time, and so the SD of RA measurements, rather than the RSD, was calculated. The SD was lowest in the experimental RP and highest in the standard RP (Table 5). The experimental RP was deepest relative to the reference ring, the Moorfields RP was less deep, and the Standard RP was the least deep.

DISCUSSION

There are several considerations regarding the choice of RP. The first consideration relates to the relative benefits of a plane anchored to the image periphery (such as the 320 RP) and one fixed at the optic disc margin (such as the standard RP). The first approach has the advantage of greater stability of the reference surface, and the second of being able to accommodate the morphologic diversity of ONHs, such as ONH tilt.

The second consideration is related to the funnel-shaped anatomy of the ONH: the slope of the cup varies with depth (gentler slope toward the ONH surface and steeper toward the lamina cribrosa), and this affects the variability of rim and cup measurements, with greater variability arising from RP movement where the rim slope is gentler. Given the changing slope of the cup border with depth in the image, the depth of the RP determines the degree of RA measurement variability—the RA SD and RSD tend to diminish with increasing RP depth. However, the slope (rim loss/time) also tends to diminish with increasing RP depth. Thus, measurement variability is not the only consideration in evaluating an RP. The purpose of imaging is to detect glaucomatous damage and progression—an RP that is perfectly stable but incapable of detecting change would not be fit for the purpose. It is the variability in relation to magnitude of true change that is important. The data presented show that although the experimental RP has the lowest variability (Table 3), it also has the lowest slope of rim loss over time (Table 2). The proposed Moorfields RP has slightly higher variability (Table 3), but a higher slope of rim loss (Table 2), and consequently, the ratio of rim loss to variability (signal-to-noise; Table 4) is greater (although not statistically significantly so), indicating a greater facility to detect progression.

The experimental RP has the deepest position in the image (Table 5) and the standard and Moorfields RPs the most superficial. To take an extreme case, if the RP is below the cup, the entire disc area is calculated as the rim. Since the disc area is fixed, the rim seems unchanging, and the RP has a good measurement reproducibility. To overcome this problem, we calculated the ratio between rim loss slope and RSD (signal-to-noise) to use as an evaluation parameter for judging the various RPs.

In this study, we compared five RPs. The 320 RP height is fixed relative to the mean height of the reference ring, whereas the others are more operator-dependent, since they rely more on the manually drawn ONH margin contour line. Both approaches have advantages and disadvantages.

TABLE 3. Global RA RSD for Each RP in the Converter Group

RP	Global RSD/mm^2
Standard	0.057*
Experimental	0.035
Moorfields	0.037
320 New	0.036
320 Old	0.038

* Significantly different RSD ($P < 0.0006$) than that at the other planes (experimental $P < 0.0001$, Moorfields $P < 0.0002$, 320 New and Old $P < 0.0006$; comparison of RSD for each of the reference planes in the converter group with paired *t*-test, $P < 0.05$).

Downloaded from iovs.arvojournals.org on 06/30/2019

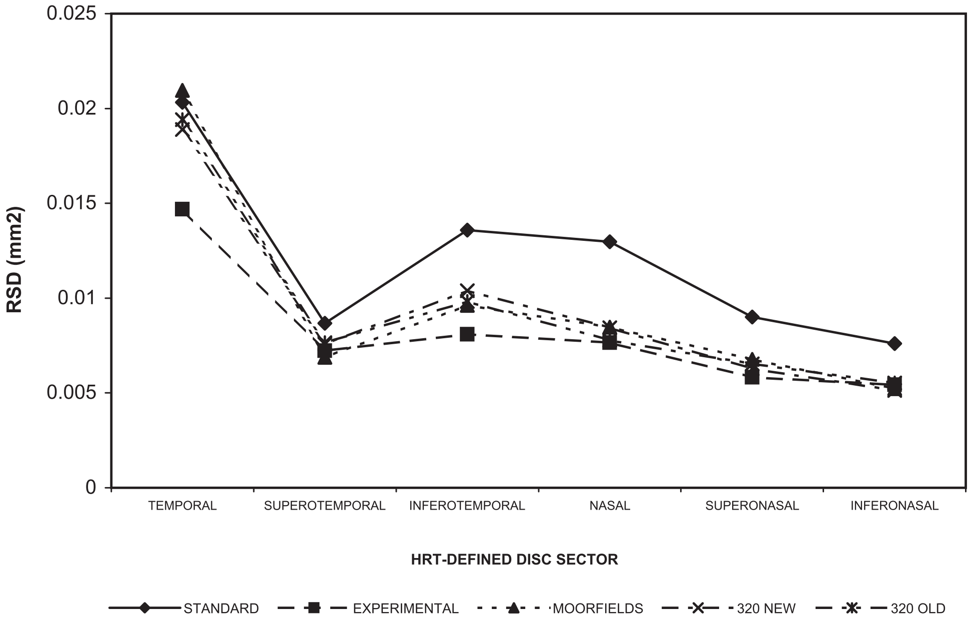

Figure 4. Sector rim area RSD for each RP in the converter group.

The 320 RP has the advantage of a remarkable stability. However, in optic discs with oblique insertion, the temporal sector RA may be underestimated. On other hand, in advanced glaucoma the thinning of retinal nerve fiber layer may cause a small posterior shift of the RP. The stability of the 320 RP has been improved further with the new HRT-3 software. In previous software versions, the reference ring was confined to regions of overlap between image pairs, with the consequence that the reference ring frequently varied in size and position through a series over time. In the HRT-3 software, the reference ring maintains a fixed size and position in the image periphery (Fig. 1).

The standard RP height is fixed relative to the height of the optic disc border and this permits an assessment of stereometric parameters that is relatively independent of the relative position of the ONH and parapapillary retinal surface (which may alter in ONH tilting). The temporal disc margin location was chosen, in part, because it was thought that the papillomacular bundle was relatively stable in thickness and affected only late in glaucoma. However, an OCT study has shown that the retinal nerve fiber layer thickness at the papillomacular bundle becomes thin in glaucoma.[34] The experimental RP was designed with the purpose of overcoming the limitations of the other RPs. It always lies below the ONH margin contour line, and it does not rely on a localized region at the ONH margin for the determination of its depth position. The experimental RP has the smallest rim loss slope and the smallest RSD. It also lies deeper, on average, in the topography, which this explains the study findings (the rim slope is steeper toward the depth of the cup, and sometimes the RP lies beneath the cup base).

The proposed Moorfields RP has been designed based on the idea of combining the stability of 320 RP with the adaptability (to individual ONHs) of the standard RP, which takes into account the morphologic variability of optic nerve heads and at the same time is linked to an anatomic region that is relatively more stable because the aforementioned changes described in macular and (presumably) papillomacular bundle. The result is that there is a trend for the Moorfields RP to provide the best slope/RSD ratio of all the RPs: This trend means that it combines good measurement reproducibility with good sensitivity to detect changes. It is particularly evident in the temporal superior and temporal inferior sectors. The differences in signal-to-noise ratio between RPs was not statistically, significant, however, and thus needs further investigation in a larger dataset. Furthermore, the clinical relevance of the finding needs to be established in independent longitudinal datasets.

It is also interesting to note the effect of the new alignment algorithm in the HRT-3 software on the performance of the 320 RP. The new alignment algorithm affords a slight improvement in RA variability (Table 3), with a minimal effect on slope of RA/time (Table 2). The higher ratio of slope:RSD (Table 4) indicates a modest improvement in the 320 RP's ability to discriminate change from measurement noise with the new alignment algorithm.

In conclusion, the Moorfields RP offers an improvement in the reproducibility of HRT stereometric parameters compared with the standard RP and, at the same time, may be more suitable for detecting change.

Table 4. Table of RA/Time Divided by RSD at Each RP in the Converter Group

RP	Slope/RSD
Standard	−0.215
Experimental	−0.268
Moorfields	−0.314
320 New	−0.274
320 Old	−0.253

Table 5. Mean Depth of Each RP and SD of RA Measurements in the Normal Group

RP	Mean Depth (mm to Reference Ring)	SD
Standard	0.204	0.054
Experimental	0.365	0.031
Moorfields	0.228	0.047
320 New	0.320	0.036
320 Old	0.320	0.037

Downloaded from iovs.arvojournals.org on 06/30/2019

References

1. Sommer A, Pollack I, Maumenee AE. Optic disc parameters and onset of glaucomatous field loss: methods and progressive changes in disc morphology. *Arch Ophthalmol*. 1980;9:1444–1448.
2. Motolko M, Drance SM. Features of the optic disc in preglaucomatous eyes. *Arch Ophthalmol*. 1981;99:1992–1994.
3. Pederson JE, Anderson DR. The mode of progressive disc cupping in ocular hypertension and glaucoma. *Arch Ophthalmol*. 1980;98: 490–495.
4. Tuulonen A, Airaksinen PJ. Initial glaucomatous optic disk and retinal nerve fiber layer abnormalities and their progression. *Am J Ophthalmol*. 1991;111:485–490.
5. Kahn HA, Leibowitz H, Ganley JP, et al. Randomized controlled clinical trial: National Eye Institute Workshop for Ophthalmologists—standardizing diagnostic procedures. *Am J Ophthalmol*. 1975;79:768–775.
6. Azuara-Blanco A, Katz LJ, Spaeth GL, et al. Clinical agreement among glaucoma experts in the detection of glaucomatous changes of the optic disk using simultaneous stereoscopic photographs. *Am J Ophthalmol*. 2003;136:949–950.
7. Zeyen T, Miglior S, Pfeiffer N, et al. Reproducibility of evaluation of optic disc change for glaucoma with stereo optic disc photographs. *Ophthalmology*. 2003;110:340–344.
8. Greaney MJ, Hoffman DC, Garway-Heath DF, Nakla M, Coleman AL, Caprioli J. Comparison of optic nerve imaging methods to distinguish normal eyes from those with glaucoma. *Invest Ophthalmol Vis Sci*. 2002;43(1):140–145.
9. Lichter PR. Variability of expert observers in evaluating the optic disc. *Trans Am Ophthalmol Soc*. 1977;74:532–572.
10. Varma R, Steinmann WC, Scott IU. Expert agreement in evaluating the optic disc for glaucoma. *Ophthalmology*. 1992;99:215–221.
11. Dreher AW, Tso PC, Weinreb RN. Reproducibility of topographic measurements of the normal and glaucomatous optic nerve head with the laser tomographic scanner. *Am J Ophthalmol*. 1991;111: 221–229.
12. Rohrschneider K, Burk RO, Kruse FE, et al. Reproducibility of the optic nerve head topography with a new laser tomographic scanning device. *Ophthalmology*. 1994;101:1044–1049.
13. Strouthidis NG, White ET, Owen VM, Ho TA, Hammond CJ, Garway-Heath DF. Factors affecting the test-retest variability of Heidelberg retina tomograph and Heidelberg retina tomograph II measurements. *Br J Ophthalmol*. 2005;89(11):1427–1432.
14. Chauhan BC, Blanchard JW, Hamilton DC, Le Balnc RP. Technique for detecting serial topographic changes in the optic disc and peripapillary retina using scanning laser tomography. *Invest Ophthalmol Vis Sci*. 2000;41:775–782.
15. Tan JCH, Hitchings RA. Optimizing and validating an approach for identifying glaucomatous change in optic nerve topography. *Invest Ophthalmol Vis Sci*. 2004;45(5):1396–1403.
16. Tan JCH, Hitchings RA. An approach for detecting glaucomatous optic nerve progression by scanning laser tomography. *Invest Ophthalmol Vis Sci*. 2003;44:2621–2626.
17. Kamal D, Garway-Heath DF, Hitchings RA, et al. Use of sequential Heidelberg retina tomograph images to identify changes at the optic disc in ocular hypertensive patients at risk of developing glaucoma. *Br J Ophthalmol*. 2000;84:993–998.
18. Kamal DS, Viswanathan AC, Garway-Heath DF, Hitchings RA, Poinoosawmy D, Bunce C. Detection of optic disc change with the Heidelberg retina tomograph before confirmed visual field change in ocular hypertensives converting to early glaucoma. *Br J Ophthalmol*. 1999;83:290–294.
19. Artes PH, Chauhan BC. Longitudinal changes in the visual field and optic disc in glaucoma. *Prog Retin Eye Res*. 2005;24(3):333–354.
20. Strouthidis NG, Scott A, Peter NM, Garway-Heath DF. Optic disc and visual field progression in ocular hypertensive subjects: detection rates, specificity, and agreement. *Invest Ophthalmol Vis Sci*. 2006;47(7):2904–2910.
21. Strouthidis NG, White ET, Owen VM, Ho TA, Garway-Heath DF. Improving the repeatability of Heidelberg retina tomograph and Heidelberg retina tomograph II rim area measurements. *Br J Ophthalmol*. 2005;89(11):1433–1437.
22. Tan JCH, Garway-Heath DF, Hitchings RA. Reasons for rim area variability in scanning laser tomography. *Invest Ophthalmol Vis Sci*. 2003;44:1126–1131.
23. Tan JCH, Garway-Heath DF, Fitzke FW, Hitchings RA. Variability across regions of the optic nerve head in scanning laser tomography. *Br J Ophthalmol*. 2003;87:557–559.
24. Owen VM, Strouthidis NG, Garway-Heath DF, Crabb DP. Measurement variability in Heidelberg Retina Tomograph imaging of neuroretinal rim area. *Invest Ophthalmol Vis Sci*. 2006;47(12):5322–5330.
25. Burk R, Vihanninjoki K, Bartke T, et al. Development of the standard reference plane for the Heidelberg Retina Tomograph. *Graefes Arch Clin Exp Ophthalmol*. 2000;238:375–384.
26. Tan JCH, Hitchings RA. Reference plane definition and reproducibility in optic nerve head images. *Invest Ophthalmol Vis Sci*. 2003;44:1132–1137.
27. Maier H, Siebert M, Gramer E, Kampik A. Eine Mebsszahl für die nervenfaserschichtdicke: messungen mit dem laser tomographic scanner (LTS). In: Gramer E, ed. Glaukom: *Diagnostic und Therapie*. Stuttgart, Germany: Enke; 1990:120–145.
28. Frohn A, Jean B, Zinser G, Thiel HJ. The problem of reference plane definition for cup volume measurements. In: Nasemann JE, Burk ROW, eds. *Laser Scanning Ophthalmoscopy and Tomography*. Munich, Germany: Quintessenz; 1990:197–206.
29. *Operation Manual for the Heidelberg Retina Tomograph Software*. Versions 1.09–2.01. Heidelberg, Germany: Heidelberg Engineering; 1993–1999.
30. Miller JM, Caprioli J. An optimal reference plane to detect glaucomatous nerve fiber layer abnormalities with computerized image analysis. *Graefes Arch Clin Exp Ophthalmol*. 1992;230:124–128.
31. Wollstein G, Garway-Heath DF, Hitchings RA. Identification of early glaucoma cases with the scanning laser ophthalmoscope. *Ophthalmology*. 1998;105(8):1557–1563.
32. Kamal D, Garway-Heath D, Ruben S, et al. Results of the betaxolol versus placebo treatment trial in ocular hypertension. *Graefes Arch Clin Exp Ophthalmol*. 2003;241(3):196–203.
33. Patterson AJ, Garway-Heath DF, Strouthidis NG, Crabb DP. A new statistical approach for quantifying change in series of retinal and optic nerve head topography images. *Invest Ophthalmol Vis Sci*. 2005;46(5):1659–1667.
34. Chen E, Gedda U, Landau I. Thinning of the papillomacular bundle in the glaucomatous eye and its influence on the reference plane of the Heidelberg retinal tomograph. *J Glaucoma*. 2001;10:386–389.

Downloaded from iovs.arvojournals.org on 06/30/2019